Understanding the role of mass transport in tuning the hydrogen evolution kinetics on gold in alkaline media

Goyal, A.; Koper, M.T.M.

Citation
Goyal, A., & Koper, M. T. M. (2021). Understanding the role of mass transport in tuning the hydrogen evolution kinetics on gold in alkaline media. *Journal Of Chemical Physics, 155*(13). doi:10.1063/5.0064330

Version:	Publisher's Version
License:	Leiden University Non-exclusive license
Downloaded from:	https://hdl.handle.net/1887/3247108

Note: To cite this publication please use the final published version (if applicable).

The Journal of Chemical Physics

Understanding the role of mass transport in tuning the hydrogen evolution kinetics on gold in alkaline media

Cite as: J. Chem. Phys. **155**, 134705 (2021); https://doi.org/10.1063/5.0064330
Submitted: 22 July 2021 . Accepted: 14 September 2021 . Published Online: 05 October 2021

Akansha Goyal and Marc T. M. Koper

COLLECTIONS

Paper published as part of the special topic on The Chemical Physics of the Electrode-Electrolyte Interface

View Online Export Citation CrossMark

ARTICLES YOU MAY BE INTERESTED IN

Classical molecular dynamics
The Journal of Chemical Physics **154**, 100401 (2021); https://doi.org/10.1063/5.0045455

Calculation of improved enthalpy and entropy of vaporization by a modified partition function in quantum cluster equilibrium theory
The Journal of Chemical Physics **155**, 104101 (2021); https://doi.org/10.1063/5.0061187

A method for calculating the nonequilibrium entropy of a flowing polymer melt via atomistic simulation
The Journal of Chemical Physics **155**, 111101 (2021); https://doi.org/10.1063/5.0056547

Challenge us.
What are your needs for periodic signal detection?
Watch

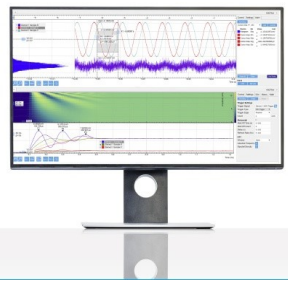

Zurich Instruments

AIP Publishing

© 2021 Author(s).

The Journal of Chemical Physics ARTICLE scitation.org/journal/jcp

Understanding the role of mass transport in tuning the hydrogen evolution kinetics on gold in alkaline media

Cite as: J. Chem. Phys. 155, 134705 (2021); doi: 10.1063/5.0064330
Submitted: 22 July 2021 • Accepted: 14 September 2021 •
Published Online: 5 October 2021

View Online Export Citation CrossMark

Akansha Goyal and Marc T. M. Koper[a)]

AFFILIATIONS

Leiden Institute of Chemistry, Leiden University, P.O. Box 9502, 2300 RA Leiden, The Netherlands

Note: This paper is part of the JCP Special Topic on The Chemical Physics of the Electrode–Electrolyte Interface.
[a)]**Author to whom correspondence should be addressed:** m.koper@chem.leidenuniv.nl

ABSTRACT

In this work, we present an in-depth study of the role of mass transport conditions in tuning the hydrogen evolution kinetics on gold by means of rotation rate control. Interestingly, we find that the hydrogen evolution reaction (HER) activity decreases with the increasing rotation rate of the electrode. As we increase the rotation (mass transport) rate, the locally generated hydroxyl ions ($2H_2O + 2e^- \rightarrow H_2 + 2OH^-$) are transported away from the electrode surface at an accelerated rate. This results in decreasing local pH and, because of the need to satisfy local electroneutrality, decreasing near-surface cation concentration. This decrease in the near-surface cation concentration results in the suppression of HER. This is because the cations near the surface play a central role in stabilizing the transition state for the rate determining Volmer step ($^*H–OH^{\delta-}–cat^+$). Furthermore, we present a detailed analytical model that qualitatively captures the observed mass transport dependence of HER solely based on the principle of electroneutrality. Finally, we also correlate the cation identity dependence of HER on gold ($Li^+ < Na^+ < K^+$) to the changes in the effective concentration of the cations in the double layer with the changes in their solvation energy.

Published under an exclusive license by AIP Publishing. https://doi.org/10.1063/5.0064330

I. INTRODUCTION

Research on the hydrogen evolution reaction (HER) in alkaline media ($2H_2O + 2e^- \rightarrow H_2 + 2OH^-$) continues to be of utmost importance for the generation of green hydrogen via alkaline water electrolysis.[1,2] Moreover, understanding the activity trends for HER is also crucial for the development of other renewable energy technologies, such as CO_2 electroreduction and electrochemical biomass upconversion, where HER can bring down the Faradaic efficiency of the process by acting as a parasitic side reaction.[3–7] Additionally, understanding the kinetic trends for this reaction is also central to our fundamental understanding of electrochemistry, since HER has long served as a model reaction for the theories and laws of electrocatalysis. In this regard, the slow kinetics of HER in alkaline media remains an active area of research, since the traditional activity descriptors fail to capture/predict the experimentally observed trends under alkaline conditions.

Traditionally, the hydrogen binding energy (HBE) on the electrocatalyst surface has been used to describe the HER kinetics in acidic electrolytes, where it successfully captures the changes in the HER activity on different metal surfaces.[8–11] However, this descriptor suffers from certain shortcomings as it not only fails to capture the experimental trends on different catalysts in alkaline media, but it also fails to explain the non-Nernstian pH dependence of HER kinetics.[12] It is now widely accepted that in order to describe the HER kinetics completely, especially under alkaline conditions, there is a need to move beyond HBE as the main descriptor and instead focus on the influence of the electrochemical environment at the metal–electrolyte interface. In fact, various groups have successfully identified different interfacial parameters, such as the interfacial field strength, the oxophilicity of the surface sites, and the cation solvation energy, to name a few, as important descriptors for the kinetics of hydrogen evolution in alkaline media.[13–16] It has been shown that these interfacial parameters can affect the HER kinetics by means of favorable/unfavorable interactions with the dissociating water molecule at the interface ($H_2O + e- + * \rightarrow H—* + OH^-$). Hence, it appears that in addition to the HBE, the interaction of the reacting water molecules and the resulting hydroxyl ions also needs

Published under an exclusive license by AIP Publishing

to be considered in order to describe the electrochemical water dissociation (Volmer step) in alkaline media completely. Eventually, a combination of different parameters may be required to accurately predict the overall HER rate.

In this light, alkali metal cations are one of the most crucial electrolyte parameters used in describing the HER kinetics in alkaline media as they can have a strong interaction with the metal surface as well as the reactants (H_2O_{ads}) and products (OH_{ads}, OH^-) of HER. Markovic and co-workers have shown that on transition metal hydroxide modified Pt electrodes, HER kinetics improves in Li^+ ion containing electrolytes, which they attribute to the stabilizing effect of Li^+ ions on the adsorbed hydroxyl ($^*OH–cat^+$) species at the interface.[17,18] However, more recently, our group as well as Tang and co-workers have shown that a direct involvement of the adsorbed hydroxyl species is not always viable under the conditions of HER (very negative overpotentials).[15,19] Instead, it is expected that cations affect the reacting water molecule at the surface by changing the barrier height for the rate determining Volmer step. In addition to the debated role of the cations in stabilizing H_2O_{ads}/OH_{ads} at the surface, it has also been shown that cations can directly adsorb at the interface (by partially losing their hydration shell), thus disrupting the $H_2O–OH_{ads}$ network and weakening the binding of OH_{ads} at the surface.[20,21] However, the exact mechanism behind the cation assisted HER in alkaline media remains disputed, as inconsistencies exist in the activity trends with cation identity on HER kinetics. It has been shown by Bandarenka and co-workers that while on Pt and Ir electrodes, the HER kinetics improves in going from CsOH < KOH < NaOH < LiOH, on Au and Ag electrodes, the opposite trend is observed.[22] Recently, we have shown that in addition to the inconsistencies in the alkali metal cation identity effects, pH affects the HER rate on Pt(111) and Au(111) electrodes differently.[23] While it was shown previously that on the Pt(111) surface, the HER activity increases in going from pH 13 to pH 11, in the case of Au(111), the opposite trend is observed. We have shown that there is a direct correlation between pH effects and cation effects for HER kinetics on gold, showing that as the electrolyte pH is increased, the near-surface cation concentration also increases due to the increasing negative charge density at the electrode. This work demonstrated the central role of cations on the kinetics of HER in alkaline media and explained, in part, the anomalous pH dependence of this reaction. Moreover, we showed that at high cation concentrations, the promotional effect of cations plateaus and eventually becomes inhibitive, which we ascribed to the blockage/crowding of the reactive surface by the near-surface cations.[24]

In this work, we study the role of mass transport in tuning the HER kinetics on polycrystalline Au electrodes by means of controlling the local pH gradients. We exploit the fact that as the mass transport conditions are enhanced, the local alkalinity at the surface is suppressed due to the accelerated transport of OH^- ions away from the electrode. Rather than a direct pH effect, we attribute the effect of mass transport on HER kinetics to a corresponding decrease in the near-surface cation concentration due to the need to satisfy the conservation of local electroneutrality. Hence, the increasing rotation rate lowers the HER activity on Au by indirectly controlling the local cation concentration at the interface, which is a central parameter in tuning HER kinetics. Moreover, we show that the rotation rate of HER is dependent on both bulk pH and cation identity. These trends underscore the lower effective concentration of Li^+ cations in the near-surface region due to their larger hydration shells. In summary, this work provides rational guidelines for selectively tuning the HER kinetics in alkaline media by carefully manipulating the near-surface electrolyte environment by means of bulk pH, cation identity, and mass transport.

II. EXPERIMENTAL METHODS

A. Chemicals

The electrolytes were prepared from H_2SO_4 (98% by wt. solution, EMSURE, Merck), $LiClO_4$ (99%, anhydrous, Alfa Aesar), $NaClO_4$ (99.99%, trace metals basis, Sigma-Aldrich), $KClO_4$ (≥99.99%, trace metals basis, Sigma-Aldrich), LiOH (99.995%, Alfa Aesar), NaOH (32% by wt. solution, analysis grade, Merck), KOH (≥99.995%, Suprapur, Merck), and ultrapure water (Milli-Q gradient, ≥18.2 MΩ cm, TOC <5 ppb). Ar (6.0 purity, Linde) and H_2 (5.0 purity, Linde) were used for purging the electrolytes.

B. General electrochemical methods

The electrochemical measurements at pH 10 to pH 12 were carried out in home-made borosilicate glass cells, and measurements at pH 13 (and higher) were carried out in a home-made PTFE cell. The reference electrode was separated from the working compartment with the help of a Luggin capillary, and the counter electrode was a Au wire (99.99% purity), unless otherwise stated. The glassware was cleaned prior to each experiment by boiling it five times in ultrapure water. When not in use, the glassware was stored in 1 g/l solution of $KMnO_4$ (acidified). Before boiling, any traces of $KMnO_4$ and MnO_2 were removed from the glassware by submerging it in a diluted solution of acidified H_2O_2 (few drops of conc. H_2SO_4 and 10–15 ml H_2O_2 in excess water) for half an hour. Before every experiment, the electrolytes were purged for ~20 min with Ar to remove any dissolved oxygen from the electrolyte. Moreover, during the measurement, Ar was also bubbled over the headspace of the electrochemical cell in order to eliminate any interference from ambient oxygen. A home-made reversible hydrogen electrode (RHE) was used as the reference electrode in all experiments. All electrochemical measurements were carried out using an Ivium Technologies (CompactStat.h standard) potentiostat and a modulated speed rotator (Pine Research). For all the CVs taken, 85% Ohmic drop compensation was performed. The Ohmic drop of the electrolyte was determined by carrying out electrochemical impedance spectroscopy (EIS) at 0.05 V (vs RHE, double-layer region). In all measurements, the working electrode was a Au polycrystalline disk in E6/E5 ChangeDisk tips embedded with a PEEK shroud (Pine Research).

TABLE I. Compositions of the electrolytes employed for the pH dependence studies of HER.

Bulk pH	[CatOH] (M) $Cat^+ = Li^+, Na^+, K^+$	[$CatClO_4$] (M) $Cat^+ = Li^+, Na^+, K^+$	Total ion concentration (M)
10	10^{-4}	9.99×10^{-2}	2×10^{-1}
11	10^{-3}	9.9×10^{-2}	2×10^{-1}
12	10^{-2}	9×10^{-2}	2×10^{-1}
13	10^{-1}	...	2×10^{-1}

Published under an exclusive license by AIP Publishing

TABLE II. Compositions of the electrolytes employed for the cation concentration dependence studies of HER.

Bulk pH	[CatOH] (M) $Cat^+ = Li^+, Na^+, K^+$	$[CatClO_4]$ (M)		Total ion concentration (M)
11	10^{-3}	$LiClO_4/NaClO_4$	5×10^{-3}	1.2×10^{-2}
			5×10^{-2}	1.02×10^{-1}
			2.5×10^{-1}	5.02×10^{-1}
			5×10^{-1}	$\approx 10^{0}$
			10^{0}	2×10^{0}
		$KClO_4$	5×10^{-3}	1.2×10^{-2}
			2.5×10^{-2}	5.2×10^{-2}
			5×10^{-2}	1.02×10^{-1}
			10^{-1}	2.02×10^{-1}
13	10^{-1}	$LiClO_4/NaClO_4$	5×10^{-3}	2.1×10^{-1}
			5×10^{-2}	3×10^{-1}
			2.5×10^{-1}	7×10^{-1}
			5×10^{-1}	1.2×10^{0}
			10^{0}	2.2×10^{0}
		$KClO_4$	5×10^{-3}	2.1×10^{-1}
			2.5×10^{-2}	2.5×10^{-1}
			5×10^{-2}	3×10^{-1}
			10^{-1}	4×10^{-1}

Before each experiment, the Au polycrystalline disk (diameter = 5 mm, Pine Instruments) was mechanically polished on Buehler micro-polishing cloth (8 in.) with decreasing sizes of diamond polishing suspension, namely, 3, 1, and 0.25 μm. Next, the disk was sonicated in ultrapure water and acetone for 10 min to remove any organic/inorganic impurities and mounted on the rotating disk electrode (RDE) tip. Thereafter, the Au polycrystalline disk was electrochemically polished in 0.1M H_2SO_4 (0.05–1.75 V vs RHE, 200 cycles at a scan rate of 1 V s^{-1}) by going to the Au oxide formation and reduction region.[25] Prior to each experiment, a characterization cyclic voltammogram (CV) of the disk was obtained in the same potential window where the electrochemical polishing was performed (at a scan rate of 50 mV s^{-1}), as shown in Fig. S5 (supplementary material). For calculating the current densities for the HER activity, the electrochemically active surface area (ECSA) of the disk was determined by calculating the charge from the reduction peak for Au oxide in the characterization CV and dividing it by the specific charge of one monolayer of Au (390 μC cm^{-2}).[25] The working electrode was then used for the electrochemical measurements.

C. Electrochemical measurements for HER activity

The studies for the pH dependence and the disk rotation rate dependence of HER were done in Ar sat. 0.1M electrolytes, as shown in Table I. Additionally, studies were done in 1 and 2M KOH containing electrolytes in a PTFE cell. The CVs were taken in the potential window of 0 to −0.65 V vs RHE at a scan rate of 25 mV s^{-1}, and the working electrode was rotated at different rotation rates (2500, 2100, 1800, 1600, 1400, and 1200 rpm) in every measurement. The rotation rate was always changed from the highest to the lowest rate to make sure that any changes in the local pH from the previous measurement do not interfere with the current measurement. Moreover, in between different measurements, the electrode was rotated at a given rotation rate for two minutes to make sure that the system had enough time to reach steady-state conditions.

All the studies on the bulk cation concentration dependence of HER were done at pH 11 (10^{-3}M CatOH) and pH 13 (0.1M CatOH) where the cation concentration was varied in the electrolyte by adjusting the concentration of $CatClO_4$, as shown in Table II. The CVs were taken in the potential window of 0 to −0.65 V vs RHE at a scan rate of 25 mV s^{-1}, and the working electrode was rotated at 2500 rpm in every measurement.

III. RESULTS AND DISCUSSION

In Fig. 1, we show that on the polycrystalline Au surface, the HER activity improves as we go from a lower rotation rate to a higher rotation rate in different alkali metal ion containing electrolytes. These results are counter-intuitive since HER under alkaline conditions proceeds via the water reduction reaction ($2H_2O + 2e^- \rightarrow H_2 + 2OH^-$) and, in principle, it should be mass transport independent. However, in addition to the enhanced mass transport of the reactants to the electrode surface, the rotation rate of the electrode also tunes the local pH gradients. It is well known that during HER, the local pH in the diffusion layer is higher compared to the bulk, both under acidic conditions (proton reduction) and under alkaline conditions (water reduction) due to proton consumption and hydroxyl ion generation, respectively.[26–28] Here, the rotating rate of the electrode tunes these gradients via the control of the diffusion layer

Published under an exclusive license by AIP Publishing

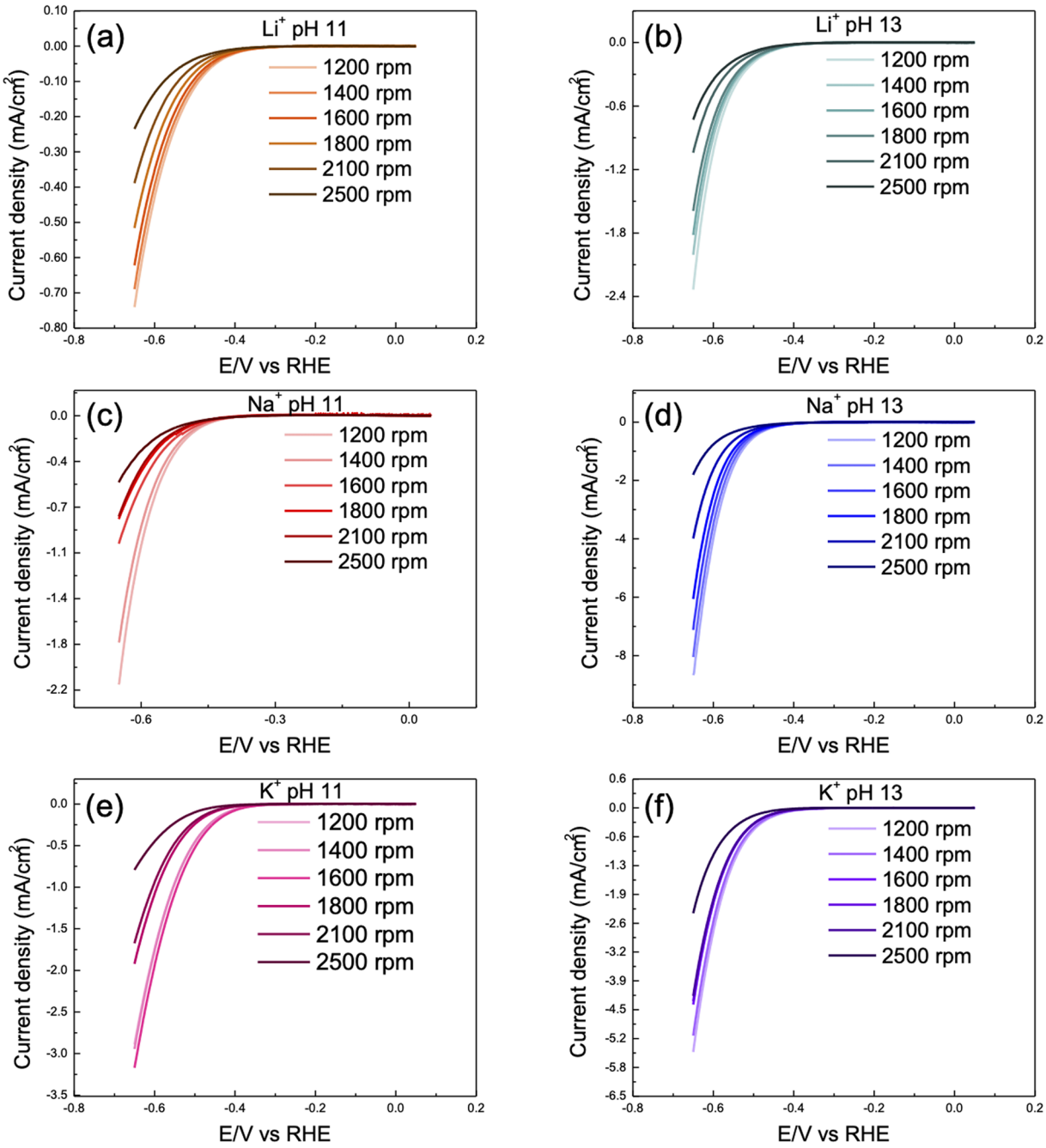

FIG. 1. Negative-going scan of the cyclic voltammograms obtained for HER on the Au polycrystalline surface in 0.1M Li^+ ion containing electrolytes at (a) pH 11 and (b) pH 13, in 0.1M Na^+ ion containing electrolytes at (c) pH 11 and (d) pH 13, and in 0.1 M K^+ ion containing electrolytes at (e) pH 11 and (f) pH 13 at a fixed cation concentration in the bulk (0.1M) at different rotation rates (2500, 2100, 1800, 1600, 1400, and 1200 rpm) at a scan rate of 25 mV s^{-1}.

thickness.[3,29] Briefly, an increasing rotation rate results in an accelerated transport of OH^- ions away from the electrode surface, thereby leading to a lower local alkalinity. Hence, the observed rotation rate dependence, as shown in Fig. 1, suggests a local pH dependence for HER on Au.

In Fig. 2, we probe this further and we find that the HER activity is indeed pH dependent. We see that it improves with increasing pH (pH 10 to pH 13) in electrolytes containing different alkali metal cations. Moreover, the Tafel slope analysis also confirms that the HER kinetics improves with the increasing bulk pH. Here, the pH

Published under an exclusive license by AIP Publishing

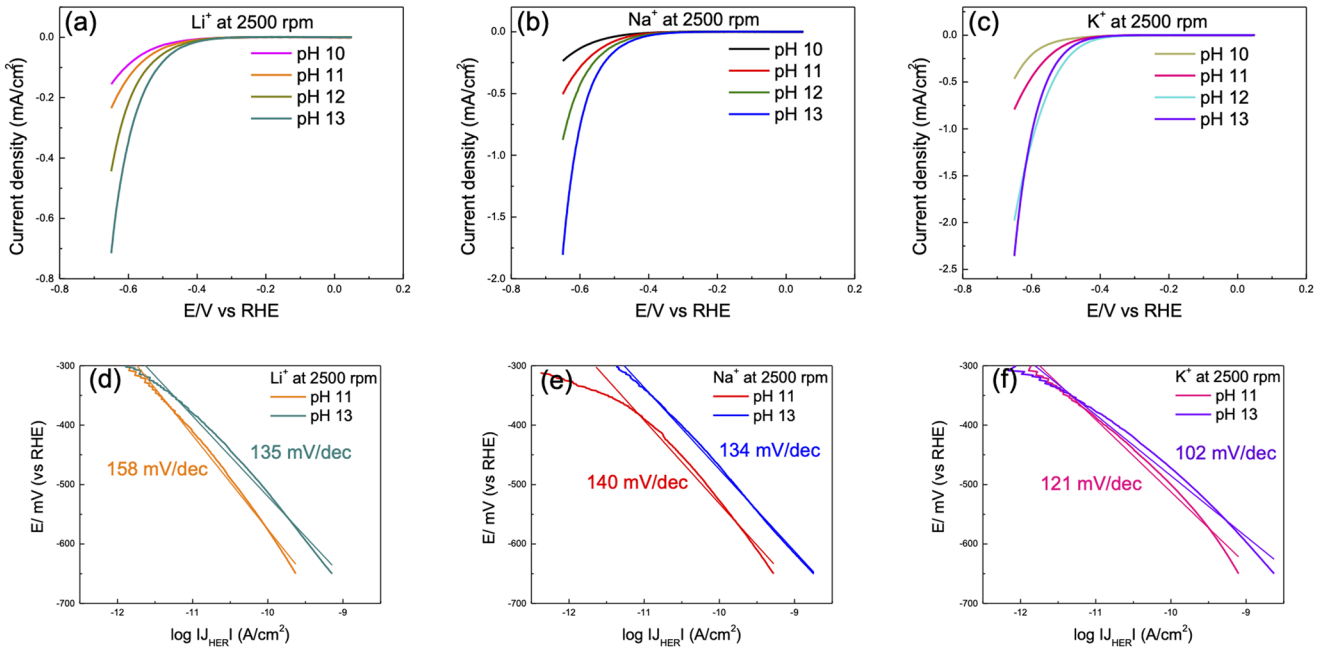

FIG. 2. Negative-going scan of the cyclic voltammograms obtained for HER on the Au polycrystalline surface in (a) Li^+, (b) Na^+, and (c) K^+ containing electrolytes at a fixed cation concentration in the bulk (0.1 M) at different electrolyte pH (pH 10, pH 11, pH 12, and pH 13) at 2500 rpm and a scan rate of 25 mV s^{-1}. The Tafel slope analysis for HER on the Au polycrystalline surface in (a) Li^+, (b) Na^+, and (c) K^+ containing electrolytes at pH 11 and pH 13, obtained from the data shown in (a)–(c).

dependence of HER kinetics agrees with our recent work where we have argued that since the potential of zero charge shifts positively (on the RHE scale) with the increasing pH ($E_{pzc} = E^{o}_{pzc} + 0.059$ pH), the interfacial electric field becomes more negative with the increasing pH at the same applied potential on the RHE scale.[30,31] Consequently, the near-surface cation concentration also increases with the electrolyte pH to counter the increasingly negative charge density at the surface (at a constant E_{RHE}/V).[23] In our recent work, we proposed that cations near the surface can enhance the HER activity on Au electrodes by favorably interacting with the transition state of the rate determining Volmer step ($H_2O + e^- + * + cat^+ \rightarrow {}^*H\text{–}OH^{\delta-}\text{–}cat^+ + (1-\delta)e^- \rightarrow {}^*H + OH^- + cat^+$).[23]

This shows that the bulk pH dependence of the HER kinetics expresses, at least in part, a dependence on the near-surface cation concentration. This can be expressed as an empirical rate law expression for HER as follows:

$$v_1 = k_1^{eff0} \exp\left(-\frac{\alpha FE}{RT}\right)\left[Cat^+\right]_s^{\gamma}, \tag{1}$$

where k_1^{eff0} is the standard rate constant, α is the transfer coefficient, F is Faraday's constant (96 485 C mol^{-1}), E is the applied potential with respect to the standard potential of the reaction, R is the universal gas constant (8.314 J K^{-1} mol^{-1}), T is the temperature (K), $[Cat^+]_s$ is the surface concentration of cations (in mol cm^{-3}), and γ is the (empirical) reaction order in the (local) cation concentration.

We note here that while the results shown in Fig. 2 capture the dependence of HER kinetics on near-surface cation concentration as a function of the bulk pH, these results still do not elucidate the local pH dependence of HER, as shown in Fig. 1. This is because the bulk pH and, hence, the interfacial electric field strength at a given potential (vs RHE) remains constant in all the measurements in Fig. 1, regardless of the rotation rate. However, in accordance with the conservation of local electroneutrality, we would expect the near-surface cation concentration to also vary with the local pH gradients even at a constant field strength. In principle, local electroneutrality will lead to a lower local cation concentration in response to a decrease in the local concentration of hydroxyl ions. Hence, increasing rotation rate will result in a corresponding lower local cation concentration due to the changes in the local pH, such that $[Cat^+]_s = [Cat^+]_b + \beta([OH^-]_s - [OH^-]_b)$ (where β is a kind of a local transference number; see Sec. S1 in the supplementary material for more details). This explains the observed suppression of HER with increasing rotation rate (as shown in Fig. 1). We can express this analytically in a simple model by assuming that under steady-state conditions, the OH^- generation rate (HER rate) must be equal to its diffusion rate,

$$k_1^{eff0} \exp\left(-\frac{\alpha FE}{RT}\right)\left(\left[Cat^+\right]_b + \beta\left(\left[OH^-\right]_s - \left[OH^-\right]_b\right)\right)^{\gamma} = \frac{D_{OH^-}}{\delta_{OH^-}}\left(\left[OH^-\right]_s - \left[OH^-\right]_b\right), \tag{2}$$

where $[OH^-]_s$ is the surface concentration of hydroxyl ions (in mol cm^{-3}), $[OH^-]_b$ is the bulk concentration of hydroxyl ions (in mol cm^{-3}), δ_{OH^-} is the diffusion layer thickness ($\delta_{OH^-} = 1.61 \times D_{OH^-}^{\frac{1}{3}} \times \nu^{\frac{1}{6}} \times \omega^{-\frac{1}{2}}$), D_{OH^-} is the diffusion coefficient of OH^-

Published under an exclusive license by AIP Publishing

(5.273×10^{-5} cm^2/s), ν is the kinematic viscosity of water (8.9×10^{-3} cm^2/s), and ω is the angular frequency of rotation (in rad/s), and the rest of the symbols have the same meaning as before. Hence, the rotation rate/mass transport rate dependence of the diffusion layer thickness (δ; calculated from the Levich equation) indirectly affects the near-surface cation concentration by controlling the local pH at the surface.

Moreover, we note here that Eqs. (1) and (2) could be rewritten to show more explicitly that the activation energy of the reaction is lowered by a factor $\gamma RT\ln(\Gamma_{cat,s}/\Gamma_{max})$ due to the presence of cations near the interface, with $\Gamma_{cat,s}$ being the surface concentration of cations in the double layer (in mol cm^{-2}) and Γ_{max} being the maximum (saturated) surface concentration of cations in the double layer.[23] It is important to distinguish between the surface concentration, which is the cation concentration just outside the double layer, and the cation concentration in the double layer, which includes the effect of cation interaction with the surface. For instance, for the same surface concentration, we expect Cs^+ to have a higher double-layer concentration than Li^+ due to its weaker hydration and stronger tendency for specific adsorption. Therefore, $\Gamma_{cat,s}$ is related to $[Cat^+]_s$ by an isotherm expression including the interaction energy between the ion and the surface.

We further studied the role of these cation interaction effects by varying the cation identity in the electrolyte. In Fig. 3 we see that the HER activity on Au electrodes increases in the order: $Li^+ < Na^+ < K^+$ under alkaline conditions (pH 11 and pH 13). Here, the cation identity trend for HER kinetics agrees well with the expected interaction strength of cations with the metal interface and the reacting water molecule. Among the different alkali metal cations, Li^+ ions tend to have the weakest interaction with the electrified interface, owing to their higher degree of solvation.[20,21,32] Moreover, Xue and co-workers have also shown previously that on the Au(111) interface, the experimentally obtained double-layer capacitance increases in going from Li^+ to Cs^+ at a fixed bulk cation concentration, suggesting that the effective double-layer concentration of the cations increases ($Li^+ < Na^+ < K^+ < Cs^+$) with the decreasing solvation energy of the cations.[33,34] Based on these results, we propose that the enhancement in the HER activity on Au electrodes in going from Li^+ to K^+ is associated with the increase in effective concentration of the cations near the surface ($\Gamma_{cat,s}$) with a lower degree of solvation.

Moreover, in Fig. 4, we plot the reaction order for HER in bulk cation concentration for different alkali metal cations at pH 11 and pH 13. At pH 11, the positive reaction order in cation concentration increases in going from $Li^+ < Na^+ < K^+$. This agrees with our hypothesis that the effective near-surface concentration of the cations depends on their hydration energy, and hence, the increase in the reaction order can be attributed to the corresponding increase in the near-surface "double-layer" cation concentration in going from Li^+ to K^+. Interestingly, we see that the reaction orders for all cations are less than 1, which indicates that the inner-layer cation concentration is approaching saturation already at intermediate pH values. Furthermore, at pH 13, we see that while in Li^+ ion containing electrolytes the reaction order in cation concentration (≈0.3) is similar to the reaction order observed at pH 11, in Na^+ and K^+ containing electrolytes, the reaction orders become negative. Moreover, the reaction order is more negative for K^+ than it is for Na^+. In fact, a closer look at the Na^+ ion containing electrolyte at pH 13 [Fig. 3(e)] shows that while an initial increase in the cation concentration shows a near-zero reaction order for HER, only at higher cation concentrations, the reaction order becomes negative [also shown in Fig. S2(b) in the supplementary material]; while in the case of K^+ ion containing electrolyte, a purely negative reaction order [Fig. 3(f)] is obtained. These results show that as the bulk electrolyte pH and thus the near-surface cation concentration increase above a threshold (saturation) concentration, the promotional effect of the cations on the HER kinetics vanishes and effectively becomes inhibitive at very high cation concentrations. Traditionally, negative reaction orders above a threshold concentration are attributed to the blocking of the reactive sites at the surface. However, it remains an active area of debate in the field whether the cations chemically adsorb at the surface or simply accumulate in the outer-Helmholtz plane in the double layer.[12,24,35] In either case, it would be expected that the accumulated cations near the surface can result in detrimental effects for HER if the cation–metal interactions are boosted at the expense of water–metal interactions. This hypothesis also explains the stronger "blocking" effect at pH 13 in K^+ ion containing

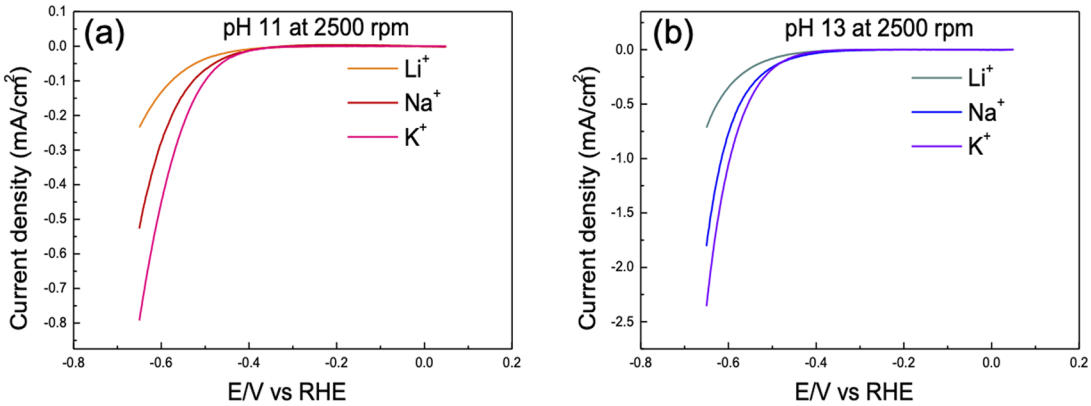

FIG. 3. Negative-going scan of the cyclic voltammograms obtained for HER on the Au polycrystalline surface for a fixed cation concentration in the bulk (0.1 M) at (a) pH 11 and (b) pH 13 at 2500 rpm and a scan rate of 25 mV s^{-1} in electrolytes containing different alkali metal cations: Li^+, Na^+, and K^+.

Published under an exclusive license by AIP Publishing

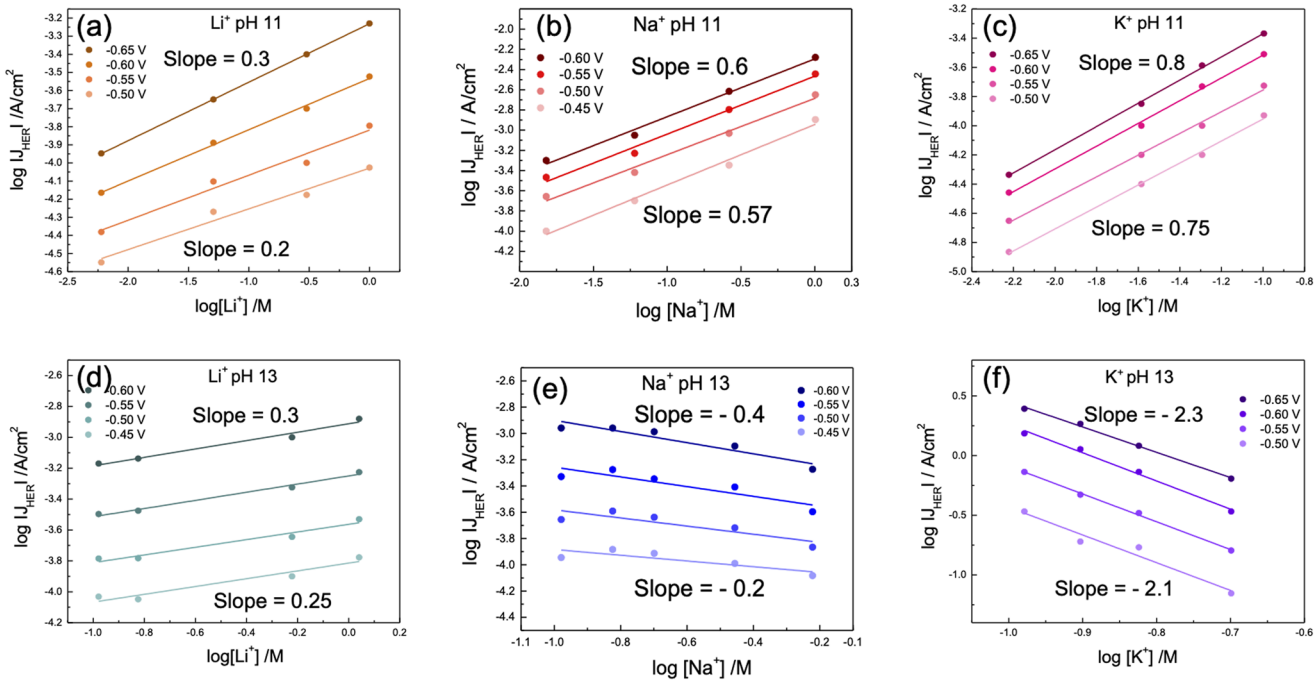

FIG. 4. Reaction order plots obtained for HER on the Au polycrystalline surface at pH 11 in (a) Li^+, (b) Na^+, and (c) K^+ ion containing electrolytes and at pH 13 in (d) Li^+, (e) Na^+, and (f) K^+ ion containing electrolytes with varying cation concentration in the bulk at 2500 rpm at a scan rate of 25 mV s^{-1} where the slope indicates the corresponding reaction order at a fixed potential (vs RHE).

electrolytes compared to Li^+ and Na^+ ion containing electrolytes, since Li^+ cations have the weakest interaction with the metal surface due to their higher degree of solvation.[20,21,24] Hence, these results suggest that intermediate electrolyte pH is optimal for the cation assisted HER mechanism in alkaline media, and more extreme near-surface cation concentrations at very high pH can lead to a diminishing HER activity as the strong cation–metal interactions render the metal surface less active for HER.

Since at extremely high pH values, K^+ ions show a negative reaction order for HER [Fig. 3(f)], we also looked at the rotation rate dependence of HER in 1 and 2M KOH containing electrolytes (Fig. 5). Interestingly, in contrast with the results obtained at lower pH values, we observe that under these conditions, an increasing rotation rate results in increasing HER activity in 1 and 2M KOH containing electrolytes. Here, the reversed rotation rate dependence confirms that at extremely high bulk pH/cation concentration

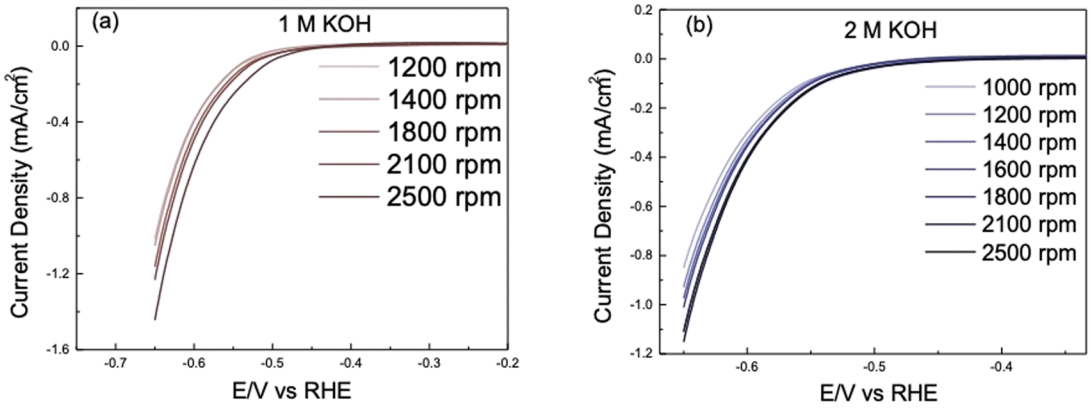

FIG. 5. Negative-going scan of the cyclic voltammograms obtained for HER on the Au polycrystalline surface in (a) 1 M KOH (pH 14) and (b) 2 M KOH at different rotation rates at a scan rate of 25 mV s^{-1}. In contrast to Figs. 4 and S3, under these conditions we find that the HER increases with increasing rotation rate, in agreement with the idea that we are in the concentration regime where the cation inhibits the HER.

Published under an exclusive license by AIP Publishing

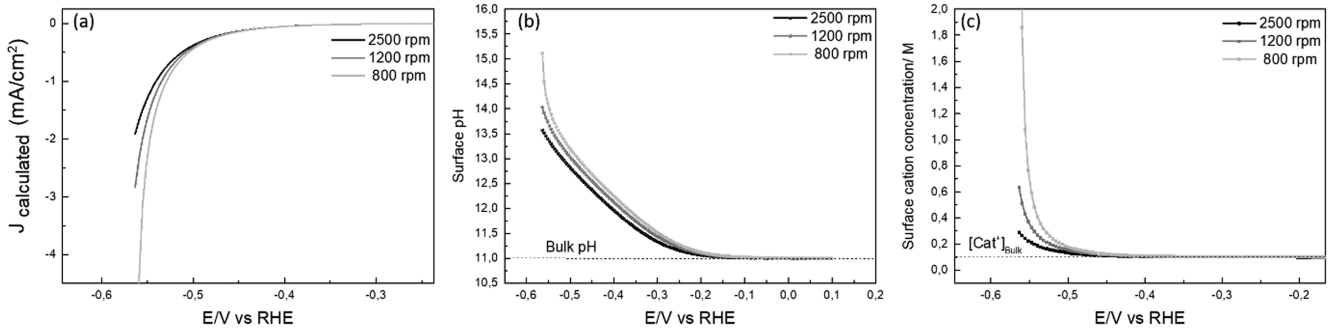

FIG. 6. (a) Simulated linear sweep voltammogram for HER on Au electrodes as obtained from Eq. (S12) (supplementary material) at different rotation rates (2500, 1200, and 800 rpm). (b) The as-calculated surface pH [Eq. (S11)] as a function of the applied overpotential (vs RHE) at different rotation rates, where the bulk pH is 11 in all the calculations. (c) The as-calculated surface cation concentration [Eq. (S7)] as a function of the applied overpotential (vs RHE) at different rotation rates, where the bulk cation concentration is 0.1 M in all the calculations.

values, an increasing near-surface cation concentration ($[Cat^+]_s$) indeed inhibits HER, and hence, lowering the local pH and thereby the local cation concentration enhances the HER rate. In the current model equations (1) and (2), this effect can be modeled by assuming a negative γ, i.e., a negative reaction order in local cation concentration.[23] However, we also note here that the reversed rotation dependence (Fig. 5) is not as prominent as the inhibitive effect of cations obtained with increasing bulk cation concentration [Figs. 3(e) and 3(f)], and we believe that this is because while the mass transport changes can regulate the local cation concentration at the interface, in order to obtain the reversed rotation dependence, we have to employ very high bulk pH/cation concentration (pH 14, 1M) to begin with. Hence, even at the highest rotation rate (2500 rpm) the local pH/cation concentration is close to pH 14/1M, and therefore, a drastic improvement in the HER activity would not be expected.

IV. SIMULATIONS FROM THE ANALYTICAL MODEL FOR HER ON Au ELECTRODES

In this section, we present the simulated J–E curves as well as the calculated surface pH and surface cation concentration, thus obtained from the equations written above, and compare them to the experimentally observed trends (see Sec. S1 in the supplementary material for more details). The model is based on the idea that the rate of HER depends on the local (interfacial) concentration of cations, since the cations interact favorably with the transition state because a (partially) negatively charged hydroxide is being split off from the reacting water molecule, which is written analytically in the form of Eq. (1) above. Moreover, the conservation of electroneutrality within the diffusion layer dictates that an increase in the concentration of OH^- at the surface must be accompanied by a corresponding increase in the concentration of cations. Hence, the rotation rate/mass transport rate dependence of the diffusion layer thickness (δ; calculated from the Levich equation) indirectly affects the near-surface cation concentration by controlling the local pH at the surface. We note here that we make certain simplifying approximations in the model (see Sec. S1 in the supplementary material for more details), and the aim here is not to reproduce our experimental results quantitatively but rather to capture the mass transport dependence of HER qualitatively. Figure 6(a) illustrates that, in agreement with our experimental results, the simulated curves indeed show an increase in the HER current densities with the decreasing rotation rate. Here, the increase in the local pH with the decreasing rotation rate [Fig. 6(b)] results in a corresponding increase in the local cation concentration [Fig. 6(c)], which in turn leads to the increase in $J_{calculated}$ with decreasing rotation. Hence, the simplified equations written on the basis of electroneutrality are able to qualitatively capture our experimental results in the low pH/cation concentration regime (pH = 11).

V. CONCLUSIONS

This work has explored the nature of mass transport effects in tuning the kinetics of HER on polycrystalline Au electrodes. We show that the HER kinetics can be selectively steered by tuning the mass transport rate for achieving the optimal near-surface electrochemical environment for HER. It is shown that with the decreasing rotation speed of the electrode (increasing diffusion layer thickness), the HER activity can be selectively enhanced on polycrystalline Au electrodes. This enhancement arises from the associated changes in the cation concentration near the interface, which is responding to local changes in OH^- concentration to conserve electroneutrality, as the rotation rate (local pH) is changed. This is because near-surface cation concentration is a central parameter in tuning the HER kinetics in alkaline media, and we propose that cations assist in the HER mechanism by stabilizing the dissociating water molecule at the surface ($^*H–OH^{\delta-}–cat^+$). Moreover, we also developed an analytical model based on electroneutrality that qualitatively captures the observed mass transport dependence of HER as an implicit function of its near-surface cation concentration dependence.

Finally, we show that the HER kinetics also improves as the bulk electrolyte pH is increased (pH 10 to pH 13) as well as with a change in the alkali metal cation identity in the electrolyte ($Li^+ < Na^+ < K^+$). We show that both of these trends are also correlated with the increase in the near-surface cation concentration, which results in the enhancement of HER. In agreement with our previous work, we show that as the electrolyte pH increases, the near-surface cation concentration also increases due to the changing interfacial electric

Published under an exclusive license by AIP Publishing

field. Moreover, as we go from Li^+ to K^+, the double-layer cation concentration increases due to the changing solvation energy of the cations.

Interestingly, the promotional effect of cations saturates above a threshold concentration and even becomes inhibitive at extreme conditions (high bulk cation concentration and low rotation at high bulk pH). We attribute this inhibitive effect to the crowding of the double layer with extremely high near-surface cation concentrations, which can, in turn, lead to the crowding/blocking of the reactive sites for HER. This has interesting implications for the alkaline water electrolyzers, as it suggests that superior HER activity can be obtained at intermediate pH values with high ionic strength electrolytes instead of using the highly corrosive extremely alkaline conditions. Moreover, our results also suggest that depending on the strength of metal–water interactions vs metal–cation interactions, divergent HER activity trends can be obtained for the same electrolyte parameters. Hence, it is important to probe the different electrode–electrolyte combinations independently in order to assess the optimal reaction conditions for HER in alkaline media on a given catalyst.

SUPPLEMENTARY MATERIAL

See the supplementary material for the detailed analytical model and additional experimental data.

ACKNOWLEDGMENTS

This work was part of the Advanced Research Center for Chemical Building Blocks (ARC CBBC) consortium, co-financed by the Netherlands Organization for Scientific Research (NWO) and Shell Global Solutions International B.V.

AUTHOR DECLARATIONS

Conflict of Interest

The authors have no conflicts to disclose.

DATA AVAILABILITY

The data that support the findings of this study are available within the article and its supplementary material.

REFERENCES

[1]H. A. Firouzjaie and W. E. Mustain, "Catalytic advantages, challenges, and priorities in alkaline membrane fuel cells," ACS Catal. **10**(1), 225–234 (2020).
[2]S. Anantharaj, S. Noda, V. R. Jothi, S. Yi, M. Driess, and P. W. Menezes, "Strategies and perspectives to catch the missing pieces in energy-efficient hydrogen evolution reaction in alkaline media," Angew. Chem., Int. Ed. **133**, 19129 (2021).
[3]A. Goyal, G. Marcandalli, V. A. Mints, and M. T. M. Koper, "Competition between CO_2 reduction and hydrogen evolution on a gold electrode under well-defined mass transport conditions," J. Am. Chem. Soc. **142**(9), 4154–4161 (2020).
[4]C. J. Bondue, M. Graf, A. Goyal, and M. T. M. Koper, "Suppression of hydrogen evolution in acidic electrolytes by electrochemical CO_2 reduction," J. Am. Chem. Soc. **143**(1), 279–285 (2021).
[5]K. Li and Y. Sun, "Electrocatalytic upgrading of biomass-derived intermediate compounds to value-added products," Chem.-Eur. J. **24**(69), 18258–18270 (2018).
[6]C. J. Bondue and M. T. M. Koper, "Electrochemical reduction of the carbonyl functional group: The importance of adsorption geometry, molecular structure, and electrode surface structure," J. Am. Chem. Soc. **141**(30), 12071–12078 (2019).
[7]U. Sanyal, J. Lopez-Ruiz, A. B. Padmaperuma, J. Holladay, and O. Y. Gutiérrez, "Electrocatalytic hydrogenation of oxygenated compounds in aqueous phase," Org. Process Res. Dev. **22**(12), 1590–1598 (2018).
[8]N. Pentland, J. O. M. Bockris, and E. Sheldon, "Hydrogen evolution reaction on copper, gold, molybdenum, palladium, rhodium, and iron," J. Electrochem. Soc. **104**(3), 182 (1957).
[9]J. Zheng, W. Sheng, Z. Zhuang, B. Xu, and Y. Yan, "Universal dependence of hydrogen oxidation and evolution reaction activity of platinum-group metals on pH and hydrogen binding energy," Sci. Adv. **2**(3), e1501602 (2016).
[10]S. Trasatti, "Work function, electronegativity, and electrochemical behaviour of metals: III. Electrolytic hydrogen evolution in acid solutions," J. Electroanal. Chem. Interfacial Electrochem. **39**(1), 163–184 (1972).
[11]R. Parsons, "The rate of electrolytic hydrogen evolution and the heat of adsorption of hydrogen," Trans. Faraday Soc. **54**, 1053–1063 (1958).
[12]L. Rebollar, S. Intikhab, N. J. Oliveira, Y. Yan, B. Xu, I. T. McCrum, J. D. Snyder, and M. H. Tang, "'Beyond adsorption' descriptors in hydrogen electrocatalysis," ACS Catal. **10**(24), 14747–14762 (2020).
[13]R. Subbaraman, D. Tripkovic, D. Strmcnik, K.-C. Chang, M. Uchimura, A. P. Paulikas, V. Stamenkovic, and N. M. Markovic, "Enhancing hydrogen evolution activity in water splitting by tailoring Li^+-$Ni(OH)_2$-Pt interfaces," Science **334**(6060), 1256–1260 (2011).
[14]I. Ledezma-Yanez, W. D. Z. Wallace, P. Sebastián-Pascual, V. Climent, J. M. Feliu, and M. T. M. Koper, "Interfacial water reorganization as a pH-dependent descriptor of the hydrogen evolution rate on platinum electrodes," Nat. Energy **2**, 17031 (2017).
[15]I. T. McCrum and M. T. M. Koper, "The role of adsorbed hydroxide in hydrogen evolution reaction kinetics on modified platinum," Nat. Energy **5**(11), 891–899 (2020).
[16]L. Rebollar, S. Intikhab, J. D. Snyder, and M. H. Tang, "Kinetic isotope effects quantify pH-sensitive water dynamics at the Pt electrode interface," J. Phys. Chem. Lett. **11**(6), 2308–2313 (2020).
[17]D. Strmcnik, K. Kodama, D. van der Vliet, J. Greeley, V. R. Stamenkovic, and N. M. Marković, "The role of non-covalent interactions in electrocatalytic fuel-cell reactions on platinum," Nat. Chem. **1**(6), 466–472 (2009).
[18]D. Strmcnik, M. Uchimura, C. Wang, R. Subbaraman, N. Danilovic, D. van der Vliet, A. P. Paulikas, V. R. Stamenkovic, and N. M. Markovic, "Improving the hydrogen oxidation reaction rate by promotion of hydroxyl adsorption," Nat. Chem. **5**(4), 300–306 (2013).
[19]L. Rebollar, S. Intikhab, J. D. Snyder, and M. H. Tang, "Determining the viability of hydroxide-mediated bifunctional HER/HOR mechanisms through single-crystal voltammetry and microkinetic modeling," J. Electrochem. Soc. **165**(15), J3209–J3221 (2018).
[20]X. Chen, I. T. McCrum, K. A. Schwarz, M. J. Janik, and M. T. M. Koper, "Co-adsorption of cations as the cause of the apparent pH dependence of hydrogen adsorption on a stepped platinum single-crystal electrode," Angew. Chem., Int. Ed. **56**(47), 15025–15029 (2017).
[21]I. T. McCrum and M. J. Janik, "pH and alkali cation effects on the Pt cyclic voltammogram explained using density functional theory," J. Phys. Chem. C **120**(1), 457–471 (2016).
[22]S. Xue, B. Garlyyev, S. Watzele, Y. Liang, J. Fichtner, M. D. Pohl, and A. S. Bandarenka, "Influence of alkali metal cations on the hydrogen evolution reaction activity of Pt, Ir, Au, and Ag electrodes in alkaline electrolytes," ChemElectroChem **5**(17), 2326–2329 (2018).
[23]A. Goyal and M. T. M. Koper, "The interrelated effect of cations and electrolyte pH on the hydrogen evolution reaction on gold electrodes in alkaline media," Angew. Chem., Int. Ed. **60**(24), 13452–13462 (2021).
[24]J. N. Mills, I. T. McCrum, and M. J. Janik, "Alkali cation specific adsorption onto fcc(111) transition metal electrodes," Phys. Chem. Chem. Phys. **16**(27), 13699–13707 (2014).
[25]M. Łukaszewski, M. Soszko, and A. Czerwiński, "Electrochemical methods of real surface area determination of noble metal electrodes—An overview," Int. J. Electrochem. Sci. **11**, 4442–4469 (2016).

Published under an exclusive license by AIP Publishing

[26]I. Katsounaros, J. C. Meier, S. O. Klemm, A. A. Topalov, P. U. Biedermann, M. Auinger, and K. J. J. Mayrhofer, "The effective surface pH during reactions at the solid–liquid interface," Electrochem. Commun. **13**(6), 634–637 (2011).
[27]H. Ooka, M. C. Figueiredo, and M. T. M. Koper, "Competition between hydrogen evolution and carbon dioxide reduction on copper electrodes in mildly acidic media," Langmuir **33**(37), 9307–9313 (2017).
[28]M. C. O. Monteiro, L. Jacobse, T. Touzalin, and M. T. M. Koper, "Mediator-free SECM for probing the diffusion layer pH with functionalized gold ultramicroelectrodes," Anal. Chem. **92**(2), 2237–2243 (2020).
[29]G. Marcandalli, A. Goyal, and M. T. M. Koper, "Electrolyte effects on the Faradaic efficiency of CO_2 reduction to CO on a gold electrode," ACS Catal. **11**(9), 4936–4945 (2021).
[30]P. Sebastián, R. Martínez-Hincapié, V. Climent, and J. M. Feliu, "Study of the Pt (111) vertical bar electrolyte interface in the region close to neutral pH solutions by the laser induced temperature jump technique," Electrochim. Acta **228**, 667–676 (2017).
[31]A. Ganassin, P. Sebastián, V. Climent, W. Schuhmann, A. S. Bandarenka, and J. Feliu, "On the pH dependence of the potential of maximum entropy of Ir(111) electrodes," Sci. Rep. **7**(1), 1246 (2017).
[32]M. C. O. Monteiro, F. Datilla, B. Hagedoorn, R. García-Muelas, N. López, and M. T. M. Koper, "Absence of CO_2 electroreduction on copper, gold and silver electrodes without cations in solution," Nat. Catal. **4**, 654 (2021).
[33]S. Xue, B. Garlyyev, A. Auer, J. Kunze-Liebhäuser, and A. S. Bandarenka, "How the nature of the alkali metal cations influences the double-layer capacitance of Cu, Au, and Pt single-crystal electrodes," J. Phys. Chem. C **124**(23), 12442–12447 (2020).
[34]B. Garlyyev, S. Xue, S. Watzele, D. Scieszka, and A. S. Bandarenka, "Influence of the nature of the alkali metal cations on the electrical double-layer capacitance of model Pt(111) and Au(111) electrodes," J. Phys. Chem. Lett. **9**(8), 1927–1930 (2018).
[35]S. Ringe, E. L. Clark, J. Resasco, A. Walton, B. Seger, A. T. Bell, and K. Chan, "Understanding cation effects in electrochemical CO_2 reduction," Energy Environ. Sci. **12**(10), 3001–3014 (2019).

Published under an exclusive license by AIP Publishing